An investigation into non-linear interaction between buckling modes

ELSEVIER

Thin-Walled Structures **19** (1994) 129–145

0263-8231/94/$7.00

An Investigation into Non-Linear Interaction Between Buckling Modes

C. M. Menken,[a] R. Kouhia[b] & W. J. Groot[a]

[a]Eindhoven University of Technology, Faculty of Mechanical Engineering, P.O. Box 513, 5600 MB Eindhoven, The Netherlands
[b]Helsinki University of Technology, Department of Structural Engineering, Rakentajanaukio, 4A, SF-02150 Espoo, Finland

ABSTRACT

This paper is a contribution to the understanding of the interaction between overall lateral–torsional buckling and local buckling of a beam under transverse loading. It concentrates on the case where the critical load for local buckling is smallest. Three approaches have been used: numerical analysis using the asymptotic theory; a qualitative analysis using an a priori simple discrete model; and experiments. The study suggests that just three modes in the asymptotic analysis are adequate to describe the interactive behaviour. The resulting reduced potential energy expression is quite similar to that of the a priori *simple discrete model and provides insight into the destabilizing phenomenon. The experiments confirm these results.*

NOTATION

a	One third of the web height in simple discrete model
a_i	Amplitude of ith buckling mode
A_{ij}	Second-order coefficients in V
A_{ijk}	Third-order coefficients in V
A_{ijkl}	Fourth-order coefficients in V
b	Flange width
d	Length of link
E	Spring stiffness/Young's modulus
$\mathbf{f}_{ij}$	Load vector when determining second-order fields
$\mathbf{G}$	Geometric stiffness matrix

h	Web height
k	Stiffness of precompressed spring
$\mathbf{K}$	Linear stiffness matrix
l	Length
M	Number of modes in the expansion
$\mathbf{M}$	Constraint matrix
$\mathbf{p}_{ij}$	Vector containing Lagrange multipliers
P	Conservative point load
P_L	Critical load for local buckling
P_0	Critical load for overall buckling
P_p	Value of the perturbation load
q_i	Increment of Q_i, $i = 1, \ldots, 4$
Q_1	Rotation representing torsion
Q_2	Rotation representing vertical deflection
Q_3	Rotation representing lateral deflection
Q_4	Shortening of original neutral axis
Q_5, Q_6	Local buckling amplitudes
S_t	Torsional stiffness
$\mathbf{u}_i$	ith buckling mode
$\Delta\mathbf{u}$	Initial post-buckling field
$\mathbf{u}_{ij}$	Second-order field
u_0	Precompression of springs
V	Potential energy
λ	Load parameter
λ_i	ith critical value of λ
λ_p	Perturbation value of λ

1 INTRODUCTION

Non-linear interactions between buckling modes, representing one type of coupled instabilities of structures, are important from a practical point of view since if these occur, the post-buckling response may differ significantly from the uncoupled situation. Koiter was the first to formulate a general asymptotic theory of mode interactions for continua.[1] He established that mode interactions have a destabilizing influence, which for certain types of structure gives rise to a significant reduction in the load-bearing capacity. This in turn explained the discrepancy between critical loads obtained from bifurcation theory and critical loads observed in experiments, particularly for shells. This approach provided a strongly reduced potential energy function, the variables being the amplitudes of

the relevant buckling modes. A comparable theory was independently developed by Thompson and Hunt for *a priori* discrete systems.[2]

In comparison with the widely used continuation procedure, the asymptotic approach can provide some additional information such as the shape of the worst imperfection; it also enables classification of the buckling problem in terms of catastrophe theory as described, for example, by Thompson and Hunt,[3] thereby giving insight into the mechanism of the non-linear mode interaction. This paper is an attempt to add to this insight.

In the original theory, the number of discrete equilibrium equations derived from the reduced potential energy expression equalled the multiplicity of the buckling load. Early analytical investigations concentrated predominantly on the interaction between local and overall buckling for compressed structural members; consequently, the number of discrete equilibrium equations in most cases was two.[4]

However, when combining the asymptotic approach with a finite element discretization, many critical loads are involved.[5] Koiter suggested a method of handling nearly coincident critical loads, while Byskov and Hutchinson presented a formulation for well-separated critical loads.[6] It has also been shown experimentally that interaction between well-separated critical loads can occur.[7]

These developments prompted us to investigate which buckling modes are relevant for describing the post-buckling behaviour correctly. It is surmised that a limited number of modes might suffice, an idea which is supported by the following statement of Potier-Ferry:[8] 'The most typical feature of instability theory is that its fundamental characteristics can be found in very simple models. Moreover, any complicated structural system is equivalent in some sense to one of these simple models, at least in the neighbourhood of a critical state'.

A finite element program for determining the initial post-buckling behaviour of folded plate structures under arbitrary load distribution is being developed. Using this program, the rarely investigated interaction between overall lateral–torsional buckling and local buckling for beams under transverse loading is being explored. In addition, a simple discrete model has been analysed and experiments have been carried out. The present study is limited to the case where the critical load pertaining to local buckling is smaller than the critical load for overall buckling.

2 AN OUTLINE OF THE ASYMPTOTIC APPROACH

A finite element program is being developed for the initial post-buckling analysis of elastic prismatic plate structures under conservative loading,

controlled by a single loading parameter λ. The plate elements are based on the Kirchhoff plate theory. The formulation of Byskov and Hutchinson has been used, since it is known that even modes pertaining to well-separated critical loads may lead to interaction.[7,9] For additional details on the asymptotic approach, see Refs 5, 10 and 11.

The system is described by a potential energy expression that is expanded up to and including fourth-order displacements terms. Bifurcation points are characterized by the vanishing of the quadratic terms of the potential energy. Thus the first numerical step involves the solution of the linear, generalized eigenvalue problem

$$(\mathbf{K} + \lambda_i \mathbf{G})\mathbf{u}_i = \mathbf{0} \tag{1}$$

and provides a (pre-selected) number of critical loads λ_i and pertinent buckling modes $\mathbf{u}_i$.

According to the asymptotic theory, the initial post-buckling field $\Delta\mathbf{u}$ can be written as

$$\Delta\mathbf{u} = a_i\mathbf{u}_i + a_i a_j \mathbf{u}(\lambda)_{ij} \tag{2}$$

where the second-order fields $\mathbf{u}_{ij}$ and the amplitudes a_i have still to be determined. It is assumed that the contribution of the second-order fields is small in comparison with the first-order contribution. Koiter's original formulation was based on coinciding critical loads. All pertinent modes should be inserted into eqn (2). Thus, theoretically, there was no problem of choice. The same held for the (semi)analytical analyses of uniformly compressed structural members, where at least two, sometimes three, sinusoidal modes were taken into account *a priori*. In a more general finite element analysis, however, a whole spectrum of critical loads may occur, and the question arises as to which modes should be put in the linear part of the post-buckling field. This question will be discussed later.

The second numerical step involves determination of the second-order fields $\mathbf{u}_{ij}$ at fixed amplitudes a_i and expansion load λ_p. Usually an orthogonality condition

$$\mathbf{u}_k^T \mathbf{K} \mathbf{u}_{ij} = \mathbf{0} \tag{3}$$

between the modes $\mathbf{u}_k$ and the second-order fields $\mathbf{u}_{ij}$ is imposed. This constraint is conveniently taken into account by means of Lagrange multipliers. The requirement that the resulting Lagrangian functional be stationary leads to the following linear equation system:

$$\begin{bmatrix} \mathbf{K} + \lambda_p \mathbf{G} & \mathbf{M} \\ \mathbf{M}^T & \mathbf{0} \end{bmatrix} \begin{bmatrix} \mathbf{u}_{ij} \\ \mathbf{p}_{ij} \end{bmatrix} = \begin{bmatrix} \mathbf{f}_{ij} \\ \mathbf{0} \end{bmatrix} \tag{4}$$

where the vectors $\mathbf{p}_{ij}$ contain the Lagrange multipliers; the constraint matrix $\mathbf{M}$ and the 'load vectors' $\mathbf{f}_{ij}$ result from the potential energy expression now augmented with cubic and quartic terms. The appearance of the stability matrix $\mathbf{K} + \lambda_p \mathbf{G}$ in this set of equations indicates that the solution requires specific care if the perturbation load factor λ_p is close to some of the critical loads λ_i. Relevant problems in the solution of system (4) will be addressed elsewhere.[12] Once the second-order fields have been obtained, the potential energy is only a function of the amp itudes a_i and the load parameter λ, and looks like

$$V[a_i; \lambda] = \frac{1}{2} \sum_{I=1}^{M} \left(1 - \frac{\lambda}{\lambda_I}\right) a_I a_I + A_{ijk} a_i a_j a_k + A_{ijkl} a_i a_j a_k a_l \tag{5}$$

The third step involves solution of the equilibrium (amplitude) equations generated from eqn (5). Koiter described how the direction of the equilibrium path with the steepest descent or smallest rise could be found.[10]

If it is admissible to insert a small number of modes into eqn (2) in the case of a general FE post-buckling analysis, the FE model, initially comprising many degrees of freedom, would be reduced to a very simple model also described by eqn (5). This could correspond to the aforementioned statement of Potier-Ferry. The simple model would make the initially complicated model more tractable for interpretation; the mixed coefficients A_{ijk} and/or A_{ijkl}, for instance, indicate whether there is coupling between buckling modes or not. As will be demonstrated in the section on the simple discrete model, the modes that are involved in buckling may not be restricted to the modes inserted into the linear part of eqn (2), but the second-order fields $\mathbf{u}_{ij}$ may also contain relevant buckling modes.

3 NUMERICAL ANALYSIS

A simply supported aluminium ($E = 70$ GPa, $\nu = 0{\cdot}3$) T-beam was analysed as a test case. The dimensions of the cross-section are presented in Fig. 1, and were chosen such that for the shorter beams local flange buckling would occur first, while buckling is initiated by an overall lateral–torsional mode for the longer ones. Dimensioning of this beam was based on estimates of the behaviour by assuming distortion-free lateral–torsional buckling and sinusoidal local buckling. Since the local buckling load is strongly influenced by the free width of the flange, the overlap between flange and web consisted of orthotropic elements having

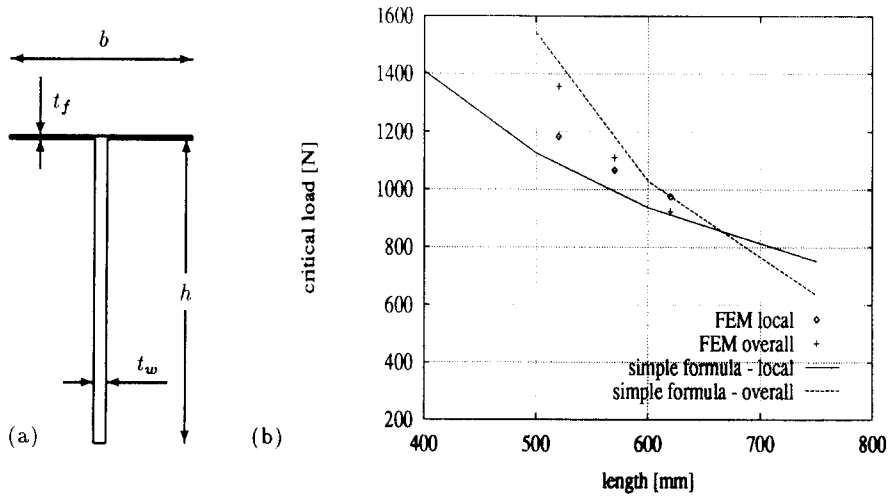

Fig. 1. (a) Cross-section; $h = 50$ mm, $b = 30$ mm, $t_f = 0{\cdot}5$ mm, $t_w = 2{\cdot}0$ mm. (b) Estimated buckling loads and the results of finite element computations.

a high rigidity in the transverse direction. The beam was loaded by a transverse force at midspan and in a direction that induced compression in the flange.

Two beams having lengths of 520 and 570 mm were modelled, and the computed buckling loads are shown in Tables 1 and 2. It is obvious that the lowest mode must be taken into account for describing the post-buckling behaviour of a perfect structure. If one looks only at the magnitude of the critical loads, at least the second mode could linearly contribute to the post-buckling field and the other modes would be 'passive', in the language of Thompson and Hunt. Tables 1 and 2, however, show the symmetry properties of the local modes too. From

TABLE 1
Lowest Buckling Modes of the 520 mm Long T-Beam

Mode no.	*Load*	*Type of mode*	*Symmetry properties with respect to*	
			Midspan	*Web*
1	1183 N	Local	Symmetric	Asymmetric
2	1184 N	Local	Asymmetric	Asymmetric
3	1211 N	Local	Symmetric	Symmetric
4	1212 N	Local	Asymmetric	Symmetric
5	1331 N	Local	Asymmetric	Asymmetric
6	1331 N	Local	Symmetric	Asymmetric
7	1356 N	Overall	Symmetric	

TABLE 2
Lowest Buckling Modes of the 570 mm Long T-Beam.

Mode no.	*Load*	*Type of mode*	*Symmetry properties with respect to*	
			Midspan	*Web*
1	1067 N	Local	Symmetric	Asymmetric
2	1068 N	Local	Asymmetric	Asymmetric
3	1092 N	Local	Symmetric	Symmetric
4	1093 N	Local	Asymmetric	Symmetric
5	1110 N	Overall	Symmetric	—
6	1192 N	Local	Asymmetric	Asymmetric
7	1192 N	Local	Symmetric	Asymmetric

previous experiments (in pure bending) and the simple discrete model (with two coinciding local critical loads), it is known that local flange buckling triggered overall lateral–torsional buckling, leaving one flange half unbuckled.[7] A comparable phenomenon cannot happen by adding the second mode to the first one. Only a combination of the first and third modes can lead to a similar phenomenon. Whereas in the simple discrete model the local critical loads were assumed to have the same value, the numerical model produced a spectrum of nearly coinciding critical loads. Two different approaches were used for solving the reduced set of equilibrium equations:

(1) the small difference between the critical loads is taken into account, leading to a secondary bifurcation on a path corresponding purely to the lowest local mode;
(2) the value of the second local critical load is replaced by the value of the lowest one, leading to a compound bifurcation point.

Results of both approaches are reproduced in Fig. 2 for the case of the 520-mm beam; the results of the first approach are drawn with solid lines, while dashed lines indicate the second approach. The figure shows that the amplitudes of the asymmetric mode 1 and the symmetric mode 3 become identical, thus leaving one flange half unbuckled. The lowest and the third buckling modes are shown in Fig. 3. It is interesting to note that the interaction between the two local modes is comparable to the behaviour of the well-known Augusti model.[13]

Since overall buckling is also involved in this problem, it remains to be decided whether its critical load can be considered to be close to the lowest one or not. Strictly speaking, if mode interaction occurs, a mode pertaining to a separated critical load will be passive. On the other hand, one could consider this situation to be a perturbation of the case of coin-

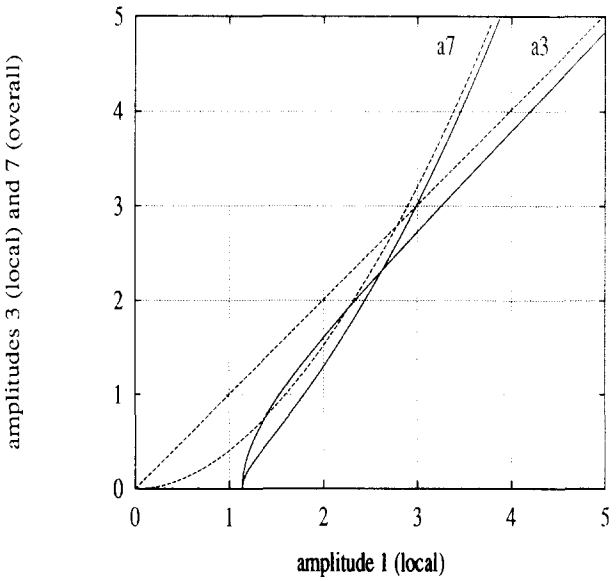

Fig. 2. The 520 mm beam; relationship between post-buckling amplitudes.

ciding critical loads. The latter approach was chosen and the overall mode was added into the linear combination, which after ignoring relatively small terms gave for the potential energy

$$V(a_1, a_3, a_i) = \frac{1}{2}\left[\left(1 - \frac{\lambda}{\lambda_1}\right)a_1^2 + \left(1 - \frac{\lambda}{\lambda_3}\right)a_3^2 + \left(1 - \frac{\lambda}{\lambda_i}\right)a_i^2\right] + A_{13i}a_1a_3a_i + A_{1111}a_1^4 + A_{1133}a_3^2 + A_{3333}a_3^4 \quad (6)$$

where i is equal to 5 for the 570-mm beam and 7 for the 520-mm beam. The cubic cross-term shows that all three modes are coupled. The deformed shape of the 520-mm beam, obtained after adding the contributions of the relevant modes, is given in Fig. 4.

4 EXPERIMENTAL VALIDATION

The numerically simulated behaviour of the aluminium T-beams was also verified experimentally. The test beams were built up from a thin flange, carefully machined from sheet metal and glued to a relatively stiff web in order to provide both flange and web with a uniform thickness. The test rig has been described earlier.[7] The dead-loading was replaced by a device for prescribing the vertical displacement at midspan. An air bearing enabled nearly frictionless lateral movement

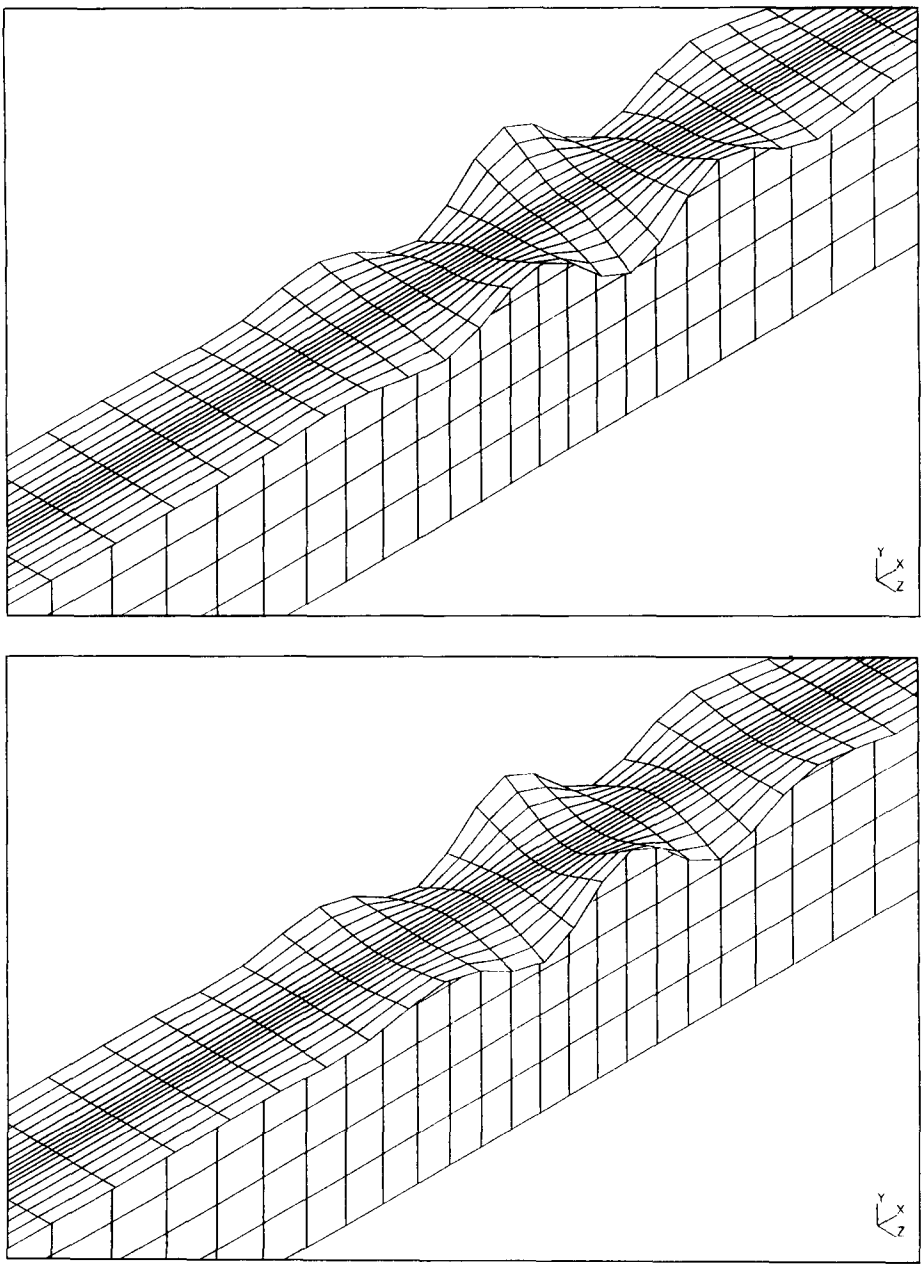

Fig. 3. Local modes 1 and 3; 520 mm beam.

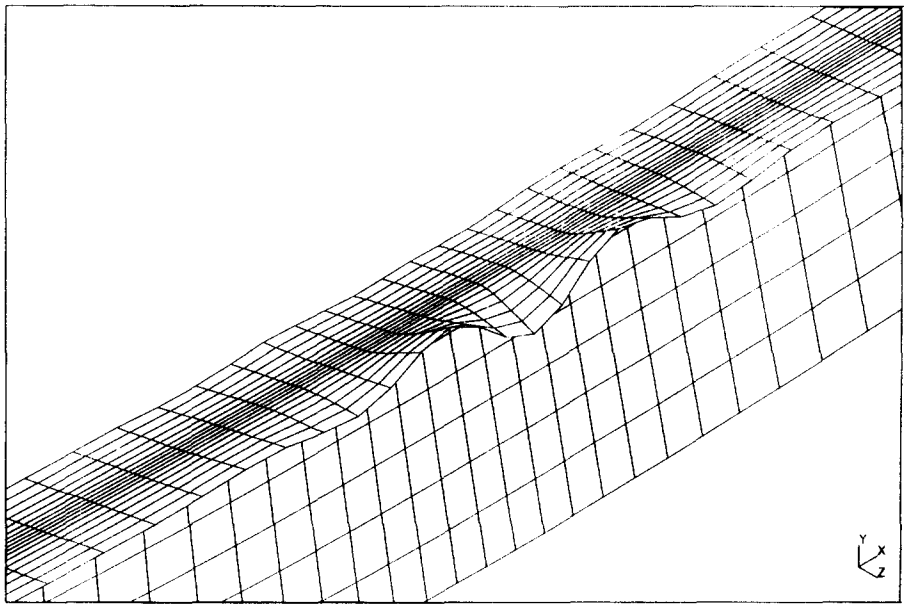

Fig. 4. Deformed shape on the post-buckling path at a load level of 1141 N, 520 mm beam, magnification ×10.

while keeping the direction of loading vertical. The overall buckling components, namely the lateral displacement of the centre of gravity of the cross-section and the rotation, were measured by means of displacement transducers at midspan. The non-periodic local buckling was measured by means of a video tracking system (Fig. 5) recording the position of an array of retro-reflective markers, glued to the rim of the flange. After processing, including subtraction of the rigid body motions of the relevant cross-sections, true local buckling properties were obtained.

Both measured and calculated values will be given in the graphs. It should be borne in mind that numerical predictions based on a perfect beam will be compared with measurements of a beam having unknown imperfections. For the shorter beams under consideration, the magnitudes of the measured overall displacements were very small. Figure 6 shows the lateral deflection of the centre of gravity at midspan representing the overall amplitude, as a function of the load. Figure 7 shows the maximum flange deflection as a function of the load. Here the influence of imperfections is less pronounced. Figure 8 shows the relationship between the maximum flange deflection and the overall amplitudes. The overall imperfections spoil the picture to some extent, but the passive behaviour of the overall mode is still discernible.

Fig. 5. Camera for measuring the non-periodic local buckle.

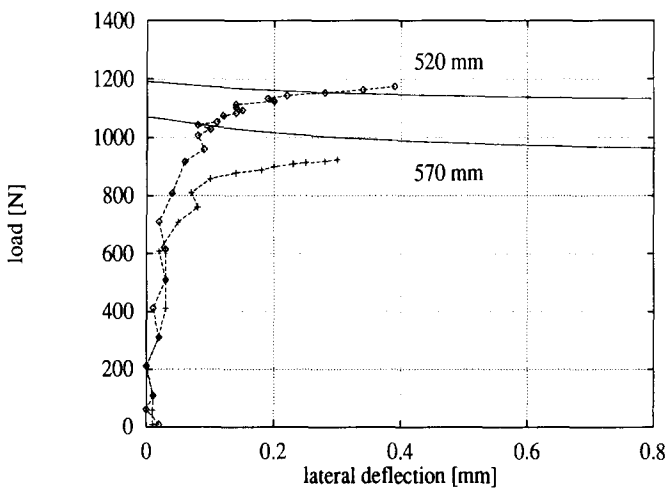

Fig. 6. Load vs lateral deflection. The solid lines are the numerical computations for a perfect beam model and the experiments are shown by lines with markers.

6 THE SIMPLE DISCRETE MODEL

A simple discrete model, Fig. 9, comprising *a priori* two coinciding local modes and one overall lateral–torsional mode was analysed to enhance

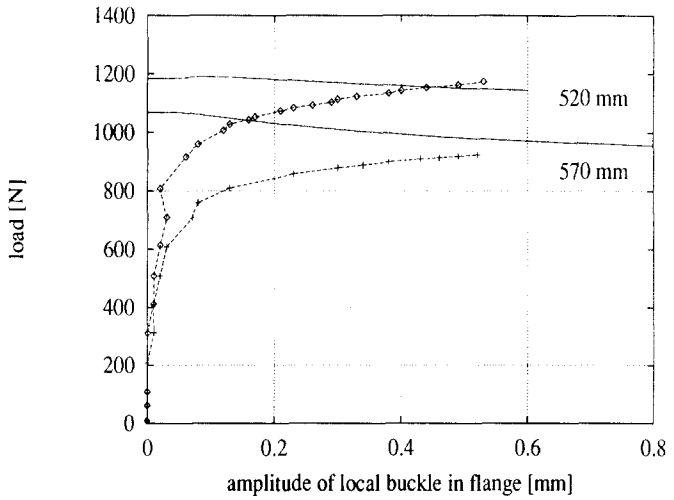

Fig. 7. Load vs maximum flange deflection. The solid lines are the numerical computations for a perfect beam model and the experiments are shown by lines with markers.

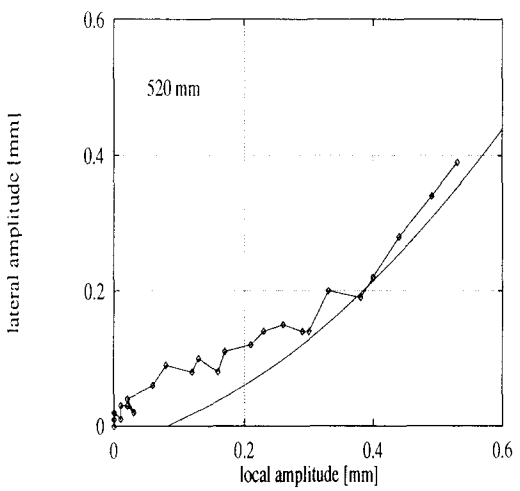

Fig. 8. Relationship between the lateral deflection and the maximum flange deflection.

insight into both the physical behaviour and the behaviour of the eqns (4) governing the second-order fields. Good qualitative agreement between this model and buckling experiments in pure bending has already been reported in Ref. 7, which also gives a more extensive description of the model. The left-hand support allowed the model to rotate about its axis, counteracted by a spring having a torsional stiffness S_t. The two linear springs, each having a stiffness E, provided the model with vertical stiff-

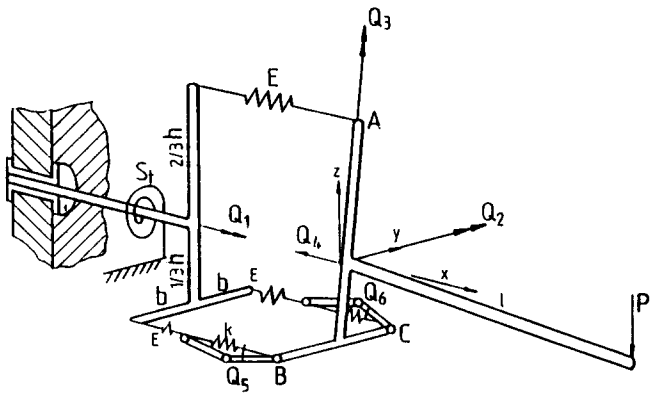

Fig. 9. Simple discrete model.

ness $\frac{2}{3}h^2E$ and lateral stiffness $2b^2E$; however, in the flanges each spring was in series with another precompressed spring, of stiffness k. The precompression u_0 was achieved by means of the rigid links. The overall lateral–torsional buckling was characterized by the rotation Q_1 and the lateral bending Q_3. The independent angles Q_5 and Q_6 characterized the local buckling of the flanges, angle q_2 representing the incremental vertical deflection, and displacement Q_4 being a shortening of the axis. The parameters were chosen in such a way that the model behaved like a real beam. The expansion of the potential energy around the fundamental state $Q_2^F = Pl/(\frac{2}{3}h^2E)$ proved to be:

$$V(Q_3, Q_5, Q_6) = \frac{1}{2}A_{33}Q_3^2 + \frac{1}{2}A_{55}Q_5^2 + \frac{1}{2}A_{66}Q_6^2 + \frac{1}{2}A_{355}Q_3Q_5^2 + \frac{1}{2}A_{366}Q_3Q_6^2 + \frac{1}{24}A_{5555}Q_5^4 + \frac{1}{4}A_{5566}Q_5^2Q_6^2 + \frac{1}{24}A_{6666}Q_6^4 \tag{7}$$

The terms $A_{355} = 2bdE$ and $A_{366} = -A_{355}$ in eqn (7) are the only ones representing coupling between lateral–torsional buckling (amplitude Q_3) and the two independent local buckling modes Q_5 and Q_6. In the previous numerical model we utilized a local mode which was symmetric with respect to the web and one which was asymmetric. This can be simulated in the simple discrete model by making

$$Q_5 = \frac{1}{2}(Q_5^* + Q_6^*) \quad Q_6 = \frac{1}{2}(Q_5^* - Q_6^*)$$

where Q_5^* causes asymmetric local buckling and Q_6^* symmetric local buckling. Then the new cubic cross-term $bdEQ_3Q_5^*Q_6^*$ will be obtained.

Next it will be shown that a second-order field may contain a passive mode, but that the accuracy of that mode will depend upon the proper choice of the perturbation load P_p. If the critical load for local buckling P_L is reached first, the coordinates Q_1, q_2, Q_3 and Q_4 will be passive. These coordinates were eliminated from the original potential energy expression still containing all coordinates (see eqn A7 in Ref. 7) by requiring the potential energy V to be stationary with respect to these passive coordinates. That gave

$$\frac{\partial V}{\partial Q_1} = 0 \Rightarrow Q_1 = -\frac{Pl}{S_t} Q_3 \tag{8}$$

$$\frac{\partial V}{\partial q_2} = 0 \Rightarrow q_2 = \frac{d}{6a} (Q_5^2 + Q_6^2) \tag{9}$$

$$\frac{\partial V}{\partial Q_3} = 0 \Rightarrow Q_3 = -\frac{A_{335}}{2A_{33}(P)} Q_5^2 - \frac{A_{366}}{2A_{33}(P)} Q_6^2 \tag{10}$$

$$\frac{\partial V}{\partial Q_4} = 0 \Rightarrow Q_4 = \frac{d}{3} (Q_5^3 + Q_6^2) \tag{11}$$

where $A_{33}(P)$ is the stability coefficient for the overall mode $(Q_1, Q_3) \neq (0, 0)$. The reduced potential energy then becomes

$$V(Q_5, Q_6) = \frac{1}{2} A_{55} Q_5^2 + \frac{1}{2} A_{66} Q_6^2 + \frac{1}{24} A_{5555}^* Q_5^4 + \frac{1}{4} A_{5566} Q_5^2 Q_6^2 + \frac{1}{24} A_{6666}^* Q_6^4 \tag{12}$$

where the new quartic coefficients can be expressed in terms of the old ones according to

$$A_{5555}^* = A_{5555} - 3 \frac{A_{355}^2}{A_{33}(P)} \tag{13}$$

The latter expression demonstrates the detstabilizing influence caused by the presence of the cubic coefficient. Now the second-order fields are determined in an analogous way to the asymptotic approach used in the numerical analysis. The active buckling modes are

$$\mathbf{u}_1^T = [0, 0, 0, 0, Q_5, 0]$$

$$\mathbf{u}_2^T = [0, 0, 0, 0, 0, Q_6]$$

The post-buckling field is described by

$$\Delta\mathbf{Q} = \mathbf{Q} + \mathbf{q} \tag{14}$$

with $\mathbf{Q} = \mathbf{u}_1 + \mathbf{u}_2$, and as $\mathbf{q}$ must be orthogonal to $\mathbf{Q}$, the second-order field looks like

$$\mathbf{q}^T = [q_1, q_2, q_3, q_4, 0, 0]$$

If this field is put into the original potential and only terms in $Q_i^n q_j$ and q_k^2 are retained, minimization of the potential energy at fixed amplitudes Q_5 and Q_6 gives

$$\begin{bmatrix} S_t & 0 & Pl & 0 \\ 0 & h^2E & 0 & 0 \\ Pl & 0 & 2b^2E & 0 \\ 0 & 0 & 0 & \frac{2}{3}E \end{bmatrix} \begin{bmatrix} q_1 \\ q_2 \\ q_3 \\ q_4 \end{bmatrix} = \begin{bmatrix} 0 \\ adE(Q_5^2 + Q_6^2) \\ -bdE(Q_5^2 - Q_6^2) \\ -dE(Q_5^2 + Q_6^2) \end{bmatrix} \tag{15}$$

which is solved at a fixed perturbation load P_p, giving

$$q_1 = -[P_p l/S_t]q_3 \qquad q_2 = [d/(6a)](Q_5^2 + Q_6^2)$$

$$q_3 = -[bdE/A_{33}(P_p)](Q_5^2 - Q_6^2) \qquad q_4 = (d/3)(Q_5^2 + Q_6^2)$$

These equations are quite similar to the ones obtained earlier and confirm that the second-order fields may contain passive modes. The only difference is that the variable load P is replaced by the fixed perturbation load P_p. For the 'incremental deflection' q_2 and the 'membrane action' Q_4, there is no difference at all. If the reduced potential energy is derived by using the relationships between active and passive coordinates, one obtains

$$V(Q_5, Q_6) = \frac{1}{2} A_{55} Q_5^2 + \frac{1}{2} A_{66} Q_6^2 + \frac{1}{24} A^{**}_{5555} Q_5^4 + \frac{1}{4} A^{**}_{5566} Q_5^2 Q_6^2 + \frac{1}{24} A^{**}_{6666} Q_6^4 \tag{16}$$

with, for instance

$$A^{**}_{5555} = A^{*}_{5555} + (P_p l)^2 \left(1 - \frac{P}{P_p}\right) \frac{A_{355}^2}{A_{33}(P_p)}$$

If the perturbation load level P_p equals the relevant load level, the coefficients will be the same.

6 CONCLUSIONS

The exploratory numerical simulations and experiments presented here confirm that it might be possible to describe with only a few buckling modes the initial post-buckling behaviour comprising non-linear mode interactions. However, selection of proper modes from the numerically obtained spectrum of modes requires insight into the buckling phenomenon at hand. The reduced potential energy expression obtained from the numerical model is very similar to that of the *a priori* simple discrete model and provides insight into the interactive buckling behaviour. The small set of non-linear equilibrium equations resulting from the numerical model can easily be solved, even providing secondary bifurcation points.

ACKNOWLEDGEMENTS

This study is supported by the Technology Foundation (STW). The authors gratefully acknowledge the contributions of R. Meerbach and R. Petterson for completing the experiments under pressure of time.

REFERENCES

1. Koiter, W. T., Over de stabiliteit van het elastisch evenwicht. PhD thesis, Delft University of Technology, Delft, The Netherlands 1945 (in Dutch). English translations: NASA TT F10, 833 (1967) and AFFDL, TR-7025 (1970).
2. Thompson, J. M. T. & Hunt, G. W., *A General Theory of Elastic Stability*. Wiley, London, UK, 1973.
3. Thompson, J. M. T. & Hunt, G. W., *Elastic Instability Phenomena*, Wiley, Chichester, UK, 1984.
4. Pignataro, M., Luongo, A. & Rizzi, N., On the effect of the local-overall interaction on the post-buckling of uniformly compressed channels. *Thin-Walled Structures*, **3** (1986) 1470–86.
5. Haftka, R. T., Mallet, R. H. & Nachbar, W., Adaptation of Koiter's method to finite element analysis of snap-through buckling behaviour. *Int. J. Solids & Structures*, **7** (1971) 1427–45.
6. Byskov, E. & Hutchinson, J. W., Mode interaction in axially stiffened cylindrical shells. *AIAA J.*, **15** (1977) 941–8.
7. Menken, C. M., Groot, W. J. & Stallenberg, G. A. J., Interactive buckling of beams in bending. *Thin-Walled Structures*, **12** (1991) 415–34.
8. Potier-Ferry, M., *Buckling and Post-Buckling*. Volume 288 of *Lecture Notes in Physics*, Springer-Verlag, Berlin, 1987, pp. 205–23.
9. Menken, C. M. & van Erp, G. M., Buckling of thin-walled beams under concentrated transverse loading. In *IUTAM Symp. on Contact Loading and*

Local Effects in Thin-Walled Plated and Shell Structures. Academia, Prague, Czechoslovakia, 1992, pp. 165–72.
10. Koiter, W. T., Current trends in the theory of buckling. In *IUTAM Symp. on Buckling of Structures*, Harvard University, Harvard, USA. Springer-Verlag, Berlin, 1974, pp. 1–16.
11. van Erp, G. M. & Menken, C. M., Initial post-buckling analysis with the spline finite strip method. *Computers and Structures*, **40** (1991) 1185–91.
12. Kouhia, R. & Menken, C. M., On the solution of second order post-buckling fields. *Commun. in Num. Meth. in Eng.*, April 1993.
13. Augusti, G., Stabilita di strutture elastiche elementari in presenza di grandi sportamenti. *Accad. Sci. Fis. Mat.*, **4**(5) (1964), Napoli, Serie 34.